Histol Histopathol (2020) 35: 395-403

http://www.hh.um.es

Histology and Histopathology

From Cell Biology to Tissue Engineering

Gap junctions and expression of Cx36 Cx43 and Cx45 in the posterodorsal medial amygdala of adult rats

Mariana Zancan[1], Taís Malysz[2,3], Dinara J. Moura[4], Ana Moira Morás[4], Luiza Steffens[4] and Alberto A. Rasia-Filho[1,3,4]

[1]Universidade Federal de Ciências da Saúde de Porto Alegre/DCBS-Physiology, [2]Universidade Federal do Rio Grande do Sul/ICBS-Anatomy, [3]Universidade Federal do Rio Grande do Sul/Graduate Program in Neurosciences and [4]Universidade Federal de Ciências da Saúde de Porto Alegre/Graduate Program in Biosciences, Porto Alegre-RS, Brazil

Summary. The posterodorsal medial amygdala (MePD) has a synaptic organization that dynamically modulates reproduction and other social behaviors in rats. Discrete gap junctions between glial cells were previously reported in the MePD neuropil. Connexins (Cx) are components of gap junctions and indicative of cellular electrical coupling. Here, we report the ultrastructural occurrence of gap junctions between neurons in the MePD and demonstrate the expression and immunofluorescent labeling of Cx36, Cx43 and Cx45 in this subcortical area of adult male rats. Few neuronal gap junctions were found in the MePD and, when identified, occurred between dendrites. On the other hand, there is a diffuse presence and distribution of punctate labelling for the tested Cxs. Puncta were visualized isolated or forming clusters in the same focal plane of cell bodies or along the MePD neuropil. The Cx36 puncta were found in neurons, Cx43 in astrocytes and Cx45 in both neurons and astrocytes. Our data indicate the presence of few gap junctions and different Cxs composition in the MePD. Because Cxs can assemble, form hemichannel units and/or serve as transcriptional regulator, it is likely that additional modulation of intercellular communication can occur besides the chemical transmission in the MePD of adult rats.

Offprint requests to: Alberto A. Rasia-Filho, UFCSPA/Fisiologia, Sarmento Leite 245, 90050-170 Porto Alegre-RS, Brazil. e-mail: rasiafilho@pq.cnpq.br, aarf@ufcspa.edu.br

DOI: 10.14670/HH-18-160

Key words: Extended amygdala, Connexin, Transmission electron microscopy, Immunofluorescence

Introduction

The posterodorsal medial amygdala (MePD) has a subpallial origin and is one of the "extended amygdala" subcortical nuclei in the rat basal forebrain (de Olmos et al., 2004; Olucha-Bordonau et al., 2015). Two main subpopulations of subcortical multipolar neurons were reported in this area, classified as bitufted or stellate cells (Rasia-Filho et al., 2012a), with distinct embryonic origins and phenotypic expressions (Choi et al., 2005; Bupesh et al., 2011). The MePD is a highly plastic area that serves as an interface for the actions of gonadal hormones (DeVries and Simerly, 2002; Gréco et al., 2003), the sensorial processing coming from main olfactory and vomeronasal pathways (Meredith and Westberry, 2004; Pereno et al., 2011; Petrulis, 2013) or mating-related genitosensorial stimuli (Coolen et al., 1997; Pfaus and Heeb, 1997). It then densely projects to hypothalamic nuclei (Petrovich et al., 2001) for the modulation of neuroendocrine secretion and reproductive behavior in both males and females (Newman, 1999; Simerly, 2004; Rasia-Filho et al., 2012b; Hull and Rodríguez-Manzo, 2017).

The MePD receives afferent synaptic inputs whose transmission, processing, and plasticity are modulated by glutamate, GABA, histamine, serotonin, and various neuroactive peptides (Micevych et al., 1988; Rasia-Filho

et al., 2012b; Quagliotto et al., 2015 and references therein). Besides the chemical transmission, a previous ultrastructural report suggested the existence of discrete gap junctions between glial cells in the rat MePD (Brusco et al., 2014). Here, we further address the ultrastructural occurrence of gap junctions between neurons at the same time that we describe for the first time the pattern of expression of connexins (Cx) in the MePD of adult rats. In this regard, gap junctions/electrical synapses are complex multimolecular structures formed by different Cxs (Rackauskas et al., 2007; Pereda et al., 2013; Griemsmann et al., 2015; Pereda, 2016; Nagy et al., 2018). Cx36-containing gap junctions establish electrical synapses between neurons (Baude et al., 2007; Schoenfeld et al., 2014). The wide expression of Cx36 in the brain suggests that not yet discovered electrical synapses can be part of distributed neural circuits and have important functions (Connors and Long, 2004; Wang and Belousov, 2011; Nagy et al., 2018). Cx43 is the major astroglial Cx (Theis and Giaume, 2012), which occurs in coupled astrocytes (Chever et al., 2014) and co-localizes with glial fibrillary acidic protein (GFAP) in the hippocampus (Wu et al., 2015). Cx45 is present in neuronal gap junctions, primarily at "mixed" glutamatergic/electrical synapses likely between mitral/tufted cell dendrites in the olfactory bulb (Rash et al., 2005). It can be co-localized with Cx36-puncta as well as along Bergmann glial processes adjacent to Cx43-puncta in the cerebellar molecular layer (Nagy and Rash, 2017). We checked for the immunofluorescence labeling of Cx36 in neurons, Cx43 in astrocytes, and Cx45 in both neurons and astrocytes to provide additional data for the occurrence of thee constitutive proteins of gap junctions in the MePD.

Materials and methods

Animals

Adult male Wistar rats (3-month-old) were housed under standard laboratory conditions with food and water *ad libitum*, room temperature around 21°C, and a 12-h light/dark cycle (lights on at 6 h). Rats were manipulated according to international laws and guidelines for the care and use of laboratory animals (European Communities Council Directive of 24 November 1986, 86/609/EEC), and the study was approved by the Animal Ethics Committee of Federal University of Health Sciences of Porto Alegre (protocols no. 248/13 and 310/15).

Transmission electron microscopy

Tissue processing was carried out exactly as reported previously (Zancan et al., 2015). Rats (n=9) were deeply anesthetized with ketamine and xylazine (intraperitoneal injections, 80 mg/kg and 10 mg/kg, respectively). Transcardiac perfusion was carried out after heparin (1,000 IU) injection in the left ventricle using 500 ml of 2% formaldehyde and 2% glutaraldehyde in 0.1 M phosphate buffer solution (0.1 M, pH 7.4; PBS) at room temperature (RT). Peristaltic pump (Control Company, Brazil) flow was initially rapid (50 ml during the first 90 s after chest opening) and, then, slowed to last for an additional 30 min period (15 ml/min flow) to maintain tissue fine ultrastructural integrity (Tao-Cheng et al., 2007; Brusco et al., 2014).

Brains were removed and immersed in the same fixative solution for 90-150 min, rinsed in PBS, and coronally sectioned using a vibrating microtome (VT 1000S, Leica Microsystems, Germany). The MePD was identified from 3.0 to 3.4 mm posterior to the bregma, laterally to the optic tract (opt) and ventrally to the stria terminalis (Fig. 1; Paxinos and Watson, 2008). The MePD was dissected from one single 400-µm-thick coronal slice. Samples were taken from the intermediate to lateral cellular parts of the MePD. We avoided gathering data from the medial cell-sparse rim "molecular layer" close to the opt.

Each tissue block was post-fixed in the same perfusion solution for 18 h, washed in PBS and postfixed in 1% osmium tetroxide (Sigma Chemicals Co., USA) for 1 h at RT. Thereafter, sections were washed in PBS, dehydrated in a graded series of alcohol and propylene oxide (Electron Microscopy Sciences, USA), embedded in resin (Durcupan, ACM-Fluka, Switzerland), left in vacuum for 24 h, and put onto slides with resin to polymerize for 48 h at 60°C.

Ultrathin sections (65-70 nm) from the whole block containing the MePD were obtained with an ultramicrotome (Leica EM UC6, Austria). Sections were mounted on copper grids (200 mesh) and stained with 1% uranyl acetate (Merck, Germany), followed by 1% lead citrate (Merck, Germany). We examined the ultrathin sections with a transmission electron microscope (TEM; JEM-1200EX II, Jeol, Japan) operated at 80 kV. The images were recorded with a camera SIS MegaView III CCD (Germany). The cellular components of the MePD were photographed first at 6,000x magnification and then at 20,000x and 60,000x. When needed, we checked for their aspect with magnifications up to 300,000x. As a rule, we observed the gap junctions at the limit of our TEM equipment resolution. Images were saved with the maximum resolution available (at 1.42 Mpx and 24 bits per pixel).

The ultrastructural aspect of neuronal gap junctions is in accordance with the characteristic morphological features described previously (Peters et al., 1991; Pannese, 2015). Dendrites were identified by the ultrastructural aspect of mitochondria, microtubules, and agranular endoplasmic reticulum (Pannese, 2015). Gap junctions in the adult rat MePD resembled those previously described in various brain nuclei of different species (Peters et al., 1991; Horiguchi et al., 2011; Brusco et al., 2014; Fig. 2). Specifically, we looked for close membrane-to-membrane appositions between neurons. We carefully observed the aspect of the

apposed structurally symmetric cell membranes, the narrow synaptic cleft formed by an array of apparently layered aspect of tight intercalated dense and lighter lines, and a lack of dense material associated with the cytoplasmatic faces of plasma membranes (Peters et al., 1991; Pannese, 2015). In addition, the space between the apposed membranes should not be obliterated by an apparent fusion of the outer leaflets of the plasma membranes, such as a zonula occludens (Peters et al., 1991), and should not show symmetrical thick and electron-dense plaques at both sides of cytoplasmic face of the plasma membranes or fine filaments converging upon these plaques as a puncta adhaerentia (Sätzler et al., 2002; Pannese, 2015).

Immunohistochemical procedure

Rats (n=4) were deeply anesthetized as above-mentioned and perfused with 400 ml of 4% formaldehyde in PBS. Brains were submitted to post-fixation during 2 h in the same fixative solution, cryoprotected using a 30% sucrose solution diluted in PBS, and stored at 4°C for 24-48 h.

Frozen cryostat sections (10 μm thick, Leica/CM 3050S, Germany) were collected on gelatinized glass slides, fixed and permeabilized by cold acetone for 10 min and dried. Acetone was the substance that provided the best results for the MePD. Although acetone could cause extraction of Cxs and under-represent actual values, it did not lead to a failure of Cxs detection in the aimed area. Afterwards, the sections were washed with PBS and delimited with a hydrophobic barrier pen (Vector Laboratories, USA). Then, the slides were air dried once again and the samples were incubated in 10% fetal bovine serum prepared in PBS containing 0.05% Triton X-100 for 1 h at RT. Sections were washed using PBS and incubated with the following primary antibodies: rabbit monoclonal anti-Cx36 (1:200; catalog no. 701630, Thermo Fisher Scientific, USA); mouse monoclonal anti-Cx43 (1:200; catalog no. 138300, Invitrogen, USA); mouse monoclonal anti-Cx45 (1:500; catalog no. MAB3100-C, Millipore, USA); mouse monoclonal anti-βIII-tubulin conjugated with eFluor 570 (1:200; catalog code 41-4510-80, eBioscience, USA), and mouse monoclonal anti-GFAP conjugated with Alexa Fluor 488 (1:200; catalog no. 131-17719; Invitrogen, USA). βIII-tubulin served as a neuronal marker and GFAP to visualize astrocytes to test their co-localization with Cxs. All antibodies were diluted in 2% fetal bovine serum prepared in PBS containing 0.05 % Triton X-100 overnight using a shaker for gentle continuous agitation at 4°C, except for the anti-GFAP and anti-βIII-tubulin which were incubated for 2 h. After subsequent rinsing with 0.05 % Triton X-100 diluted in PBS and only PBS, sections were incubated with the following secondary antibodies for 120 min at RT: goat anti-mouse IgG3 conjugated with Alexa Fluor 555 (1:1000; catalog code ab98707, ABCAM, USA) and goat anti-rabbit IgG conjugated with Alexa Fluor 488 (1:1000; catalog code ab150077, ABCAM). After rinsing with PBS, sections were counterstained with the fluorescent dye Hoechst 33342 (4 μ/ml; catalog code H3570, Thermo Fischer) for 10 min, washed again with PBS, and covered with mounting media. Hoeschst served to identify the nuclei of both neurons and glia cells in the MePD.

The antibody specificity was checked by Western blot (data not shown). Non-specific binding of the secondary antibody was controlled by omitting the primary antibody and replacing it by PBS. No reaction was observed in this condition. The pattern of immunofluorescent expression of each studied Cx was specific in fixed tissues (validated with different methodological approaches, as depicted in Nagy and

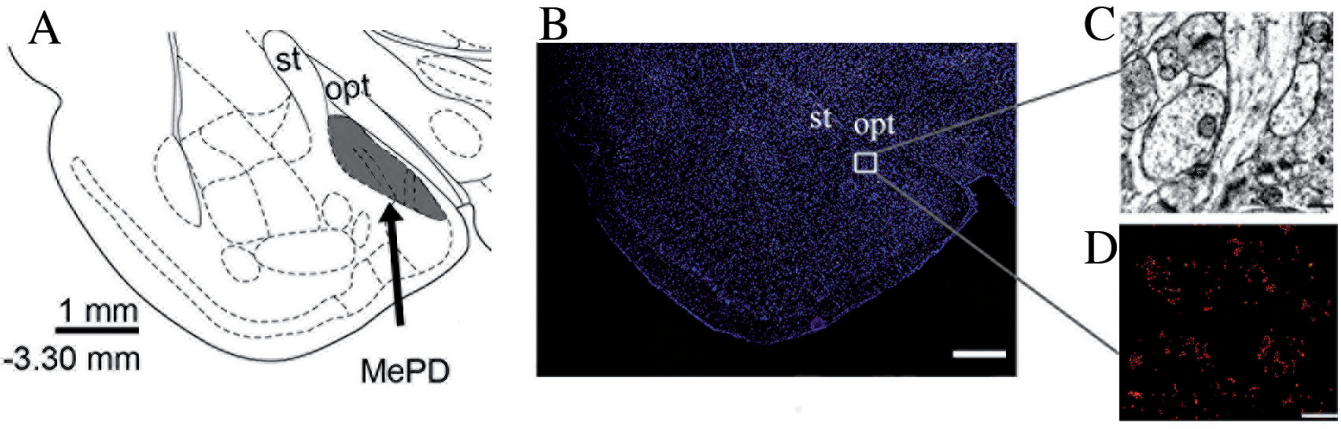

Fig. 1. A. Schematic diagram of the ventral aspect of a coronal brain section showing the posterodorsal medial amygdala (MePD, marked in gray; in this case at -3.3 mm posterior to the bregma) lateral to the optic tract (opt) and ventral to the stria terminalis (st). Adapted from Paxinos and Watson (2008). **B.** Microscopic image of a matched coronal section of the MePD to demonstrate where ultrastructural data **(C)** and immunofluorescence for connexins **(D)** were obtained. Scale bars: B, 200 μm; C, 1 μm; D, 20 μm.

Rash, 2017), following the recommendations of Saper (2005), similar to previous report (e.g., Nagy and Rash, 2017) and according to the manufacturer´s data sheet, as follows: Cx36: https://www.thermofisher.com/antibody/product/Connexin-36-Antibody-clone-12H11L18-Monoclonal/701630; Cx43: https://www.thermofisher.com/antibody/product/Connexin-43-Antibody-clone-CX-1B1-Monoclonal/13-8300; Cx45 http://www.merckmillipore.com/BR/pt/product/Anti-Connexin-45-Antibody-near-CT-cytoplasmic-clone-8A11.2-Ascites-Free,MM_NF-MAB3100-C?ReferrerURL=https%3A%2F%2Fwww.google.com.br%2F&bd=1).

The MePD was identified as described above. Images were captured using a fluorescence-inverted microscope (Olympus IX51 U-RFL-T, Olympus Corporation, USA) with plan semi-apochromat objective lens (×20, Olympus UPLFL, 0.5 N.A.). The Olympus DP controller 3.3.1292 software was used for image acquisition. At least two different images were obtained from each section, and six sections were obtained from each animal. All image acquisition procedures were held constant when gathering data for the different Cxs, βIII-tubulin, and GFAP. Hoescht was excited at 350 nm, FITC was excited at 488 nm (for βIII-tubulin and GFAP) and TRITC was excited at 555 nm (for Cx36, Cx43, and Cx45). All images had the same size (4080 x 3072 pixels). In each focal plane, results were visualized isolated or merged for the expression of: (1) Cx36 and βIII-tubulin to evaluate their concomitant presence in neurons, (2) Cx43 and GFAP to evaluate their concomitant presence in astrocytes, and (3) Cx45 and both βIII-tubulin and GFAP to evaluate their concomitant presence in neurons and astrocytes.

Images had final fine adjustments of sharpness, brightness, and contrast made in Photoshop CS3 or CS5 (Adobe Systems, USA) without altering their content.

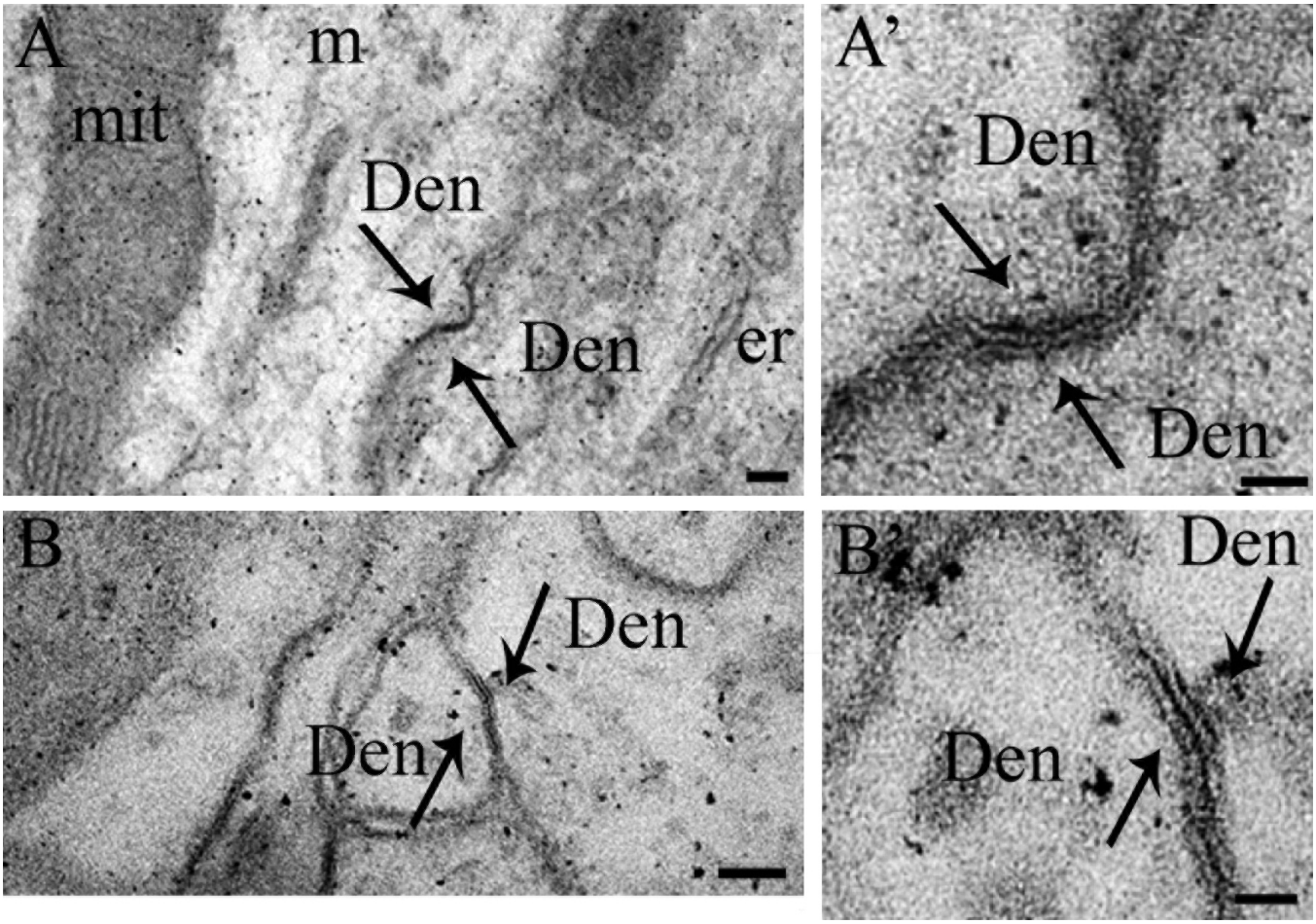

Fig. 2. A, B. Digitized electron micrographs of the ultrastructure of the posterodorsal medial amygdala of adult male rats showing a gap junction (arrow) between two dendrites. **A', B'.** Corresponding images at higher magnification. Den: dendrite; m: microtubule; mit: mitochondria; er: endoplasmic reticulum. Fine adjustments of brightness and contrast were made in Photoshop CS3 (Adobe Systems, Inc., USA). Scale bars: A, B, 70 nm; A', B', 20 nm.

Results

Scarce gap junctions between neurons were found in the MePD neuropil (Fig. 2). Few of them could be observed along several ultrathin sections from all the studied animals. We looked for such junctions between all parts of the neurons. Local gap junctions had the characteristic close apposition of cellular membranes and a narrow synaptic cleft with intercalated electron-lucent and electron-dense layers. They were identified between close neuronal segments (two dendrites), as shown in Fig. 2A,B. Empirically, we found gap junctions only between dendrites. We could not reliably observe them between cell bodies or axons.

The MePD expresses the three studied Cxs. Punctate labelling and representative images for Cx36, Cx43, and Cx45 results are shown in Fig. 3. Immunolabeled puncta were observed isolated or forming clusters. They had round or elongated aspects and were small, but usually varied in size. We identified immunfluorescent puncta in the cell body or in the neuronal and glial segments.

The immunofluorescent puncta for each Cx were visualized in the same focal plane of cell bodies and along the neuropil. For all Cxs, there were puncta that did not match exactly with the markers for neurons or glia, although it was possible to identify Cx36 puncta associated with β–III tubulin, Cx43 with GFAP, and Cx45 with both β–III tubulin and GFAP. Taking the Cx45 immunolabeling as an example, there was a consistent occurrence of puncta along neuronal and astrocytic branches. However, these puncta showed a selective distribution, i.e., there was neither a

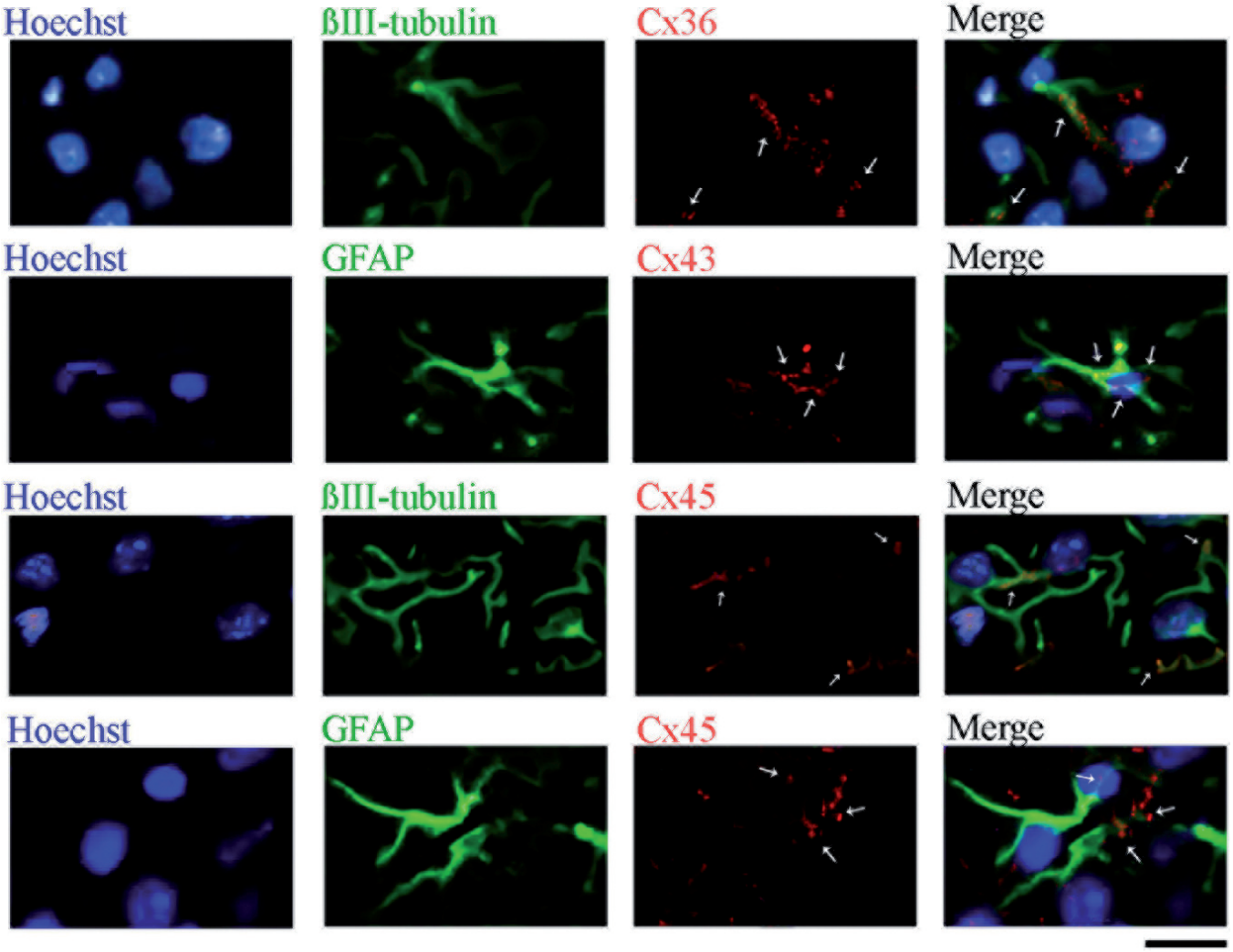

Fig. 3. Digitized images of representative immunofluorescent results for connexin (Cx) expression in the posterodorsal medial amygdala of adult male rats. Results are presented for the cell body identification (Hoechst), βIII-tubulin to identify neurons, glial fibrillary acidic protein (GFAP) to identify astrocytes, and merged corresponding images. Immunolabeled puncta for Cx36, Cx43, and Cx45 (indicated by arrows) are all present and broadly distributed in the MePD. Fine adjustments of brightness and contrast were made in Photoshop CS3 (Adobe Systems, Inc., USA). Scale bar: 20 μm.

homogenous presence of this Cx along the entire extension of a cellular process nor all branches showed the same occurrence of immunolabeled puncta in each of them.

Discussion

Our findings indicate the occurrence of gap junctions between neurons and the evident expression of Cxs in neurons and glia cells in the MePD of adult rats. The morphological and functional implications of these findings are depicted below.

First, in our samples, the search for scarce gap junctions in the MePD using TEM was a laborious procedure. This agrees with the same concern elaborated by Brusco et al. (2014), as follows: "TEM also revealed gap junctions between glial cells in the MePD neuropil. No such structures could be found on MePD neurons, either because these junctions are rare, have a restricted distribution, or have a modified structure that cannot be identified readily". We have studied adult male Wistar rats and used a similar procedure for obtaining sample sections for TEM as these authors did. There are images indicative of gap junctions on MePD neurons. Interestingly, data were obtained in a mature rat brain area whose cells and circuits retain structural and functional plasticity after critical developing periods (Rasia-Filho et al., 2012a; Zancan et al., 2015, 2018). The combination of TEM with other techniques would provide additional direct data on gap junction composition, but the total number of these gap junctions in the MePD was very low and variable within each animal and between animals that precluded additional efforts.

The reasons for the presence of gap junctions in the adult MePD are not currently known. To the best of our knowledge, there are no reports with electrophysiological recordings of electrical synapses in the MePD of adult male Wistar rats. Nevertheless, gap junctions and electrical synaptic coupling exist between neural cells in an activity-dependent manner and for cellular functional synchronization (e.g., Bennett and Zukin, 2004; Pereda et al., 2013; Nagy et al., 2018; Pernelle et al., 2018). Gap junction transmission can be modulated by the activity of the neural network and can affect awake active behaviors (Posłuszny, 2014). Coupling dendrites of adjacent neurons would provide the MePD with a possibility of compartmentalization of information processing within cellular microdomains (based on Rela and Szczupak, 2004). Some electrical coupling might also produce complex input–output functions in combination with chemical transmission (Rela and Szczupack, 2004; Langer et al., 2012; Postuszny, 2014), even that gap junctions form transient cellular ensembles (Pannasch et al., 2012; Bukalo et al., 2013; Anders et al., 2014; Pogoda et al., 2016) for short-term functional actions (Allen et al., 2011).

We found that different Cxs are expressed in the adult rat MePD, a finding that has not been addressed directly before. Rash et al. (2004), when studying the basomedial and basolateral amygdala, provided an image for the expression of Cx36 in the medial amygdala likely in its anterior aspect in mice (inferred from Fig. 5). Moderate levels of Cx36 mRNA and protein were reported in the medial amygdala of adult rats, but it is not possible to determine exactly the rostrocaudal level or the dorsoventral position where data were obtained in this nucleus and/or from a specific subnucleus (Figs. 6, 10 in Belluardo et al., 2000).

The presence of various Cx puncta contrast with the few TEM data of gap junctions in the MePD. However, the identification of Cx36 immunofluorescence is well correlated with its localization in neuronal gap junctions (Nagy et al., 2018) with electrophysiological and behavioral implications (Wang and Belousov, 2011). We found Cx36 co-expressed with βIII-tubulin in MePD neurons, as expected for the cell specificity of this Cx, suggestive of the existence of gap junctions in this brain area. In addition, Cx43 was associated with local GFAP-immunomarked astrocytes. Cx45 was detected with both βIII-tubulin and GFAP, i.e., in both neurons and astrocytes. This latter finding is interesting because Cx45 is largely absent in the adult nervous tissue, except for few brain areas (Bennett and Zukin, 2004). The rat MePD has to be included in the group of areas with Cx45 expression at adulthood as well.

The consistent expression of different Cxs in the adult MePD cells would have functional implications. We hypothesize some possibilities. For example, Cxs serve for the modulation of the dynamic cellular activity and the information processing plasticity (Nagy et al., 2018). Assembled Cxs, besides transferring ions and synchronizing activity, they can also allow the exchange of small metabolites and intracellular signaling molecules between cells (Bennett and Zukin, 2004). Cx36 binding sites also have a phosphorylation-dependent interaction and promote activation of Ca^{++}-calmodulin-dependent kinase II, which correlates with the activation of glutamate NMDA receptors associated with adjacent chemical synapses (Pereda et al., 2013). Cx43 indirectly regulates cell-cell adhesion as well as provides astrocytes with a region-specific and activity-mediated physiological heterogeneity for intercellular communication (Theis and Giaume, 2012; see additional data in Kovacs et al., 2018). Recently, it was demonstrated that Cx43 can also regulate gene transcription and N-cadherin expression (Kotini et al., 2018).

Furthermore, it has been reported that Cxs can be part of hemichannels, which can migrate in the membrane, dock and combine with other compatible Cxs to establish a contact with the apposed membrane of a neighbor cell (Pogoda et al., 2016). We can not identify specific hemichannels from our immunofluorescent data. Nevertheless, this possibility could not be dismissed when expression of different Cx are found in the MePD. Cx hemichannels can form large poorly selective pores (Tong et al., 2015), be functional units *per se*, have their

permeability modulated by phosphorylation/dephosphorylation and various cytosolic redox agents (Pogoda et al., 2016). Hemichannels-dependent ATP release promotes a signaling pathway by propagated intercellular Ca^{++} waves and activation of purinergic receptors in neighboring cells *in vitro* (Bader et al., 2012 and references therein). Hemichannels can open and connect the cell interior with the extracellular space, release and uptake diffusing ions and molecules up to 1.2 kDa, including metabolites and signaling molecules (Bader et al., 2012). For example, at least for the rat basolateral amygdala, the release of gliotransmitters through Cx43 hemichannels is necessary for memory consolidation (Stehberg et al., 2012). The occurrence of hemichannels composed by Cx in the MePD has still to be demonstrated with additional experimental approaches.

In conclusion, our findings indicate that the rat MePD has few gap junctions identified using TEM, but has an evident occurrence of immunofluorescence puncta for Cx36, Cx43 and Cx45 in local neurons and astrocytes. These morphological data address further connectional and intercellular interactions in the MePD with likely functional implications for the local neuroglial elaboration of complex social behaviors in adult rats.

Acknowledgements. Authors are thankful to Mr. Martin Ian Maher and Dr. Luis Miguel Garcia-Segura (Instituto Cajal, C.S.I.C., Madrid, Spain) for the ultrastructural images and for the critical reading of the manuscript. Grants from Brazilian Agency National Council for Scientific and Technological Development to MZ and AARF (CNPq; no. 141867/2015- 9 and 6594/2016-1) and CAPES.

Conflict of Interest. The authors declare no conflict of interest regarding the present project and results.

Role of authors. All authors contributed to study concept and design, analysis and interpretation of data, and critical revision of the manuscript. Acquisition of immunofluorescent data: MZ, DJM, AMM, and LS.

References

Allen K., Fuchs E.C., Jaschonek H., Bannerman D.M. and Monyer H. (2011). Gap junctions between interneurons are required for normal spatial coding in the hippocampus and short-term spatial memory. J. Neurosci. 31, 6542-6552.

Anders S., Minge D., Griemsmann S., Herde M.K., Steinhäuser C. and Henneberger C. (2014). Spatial properties of astrocyte gap junction coupling in the rat hippocampus, Phil. Trans. Royal Soc. B: Biol. Sci. 369, 20130600.

Bader P., Weingart R. and Egger M. (2012). Regulation of Cx45 hemichannels mediated by extracellular and intracellular calcium. Pflugers Arch. 464, 249-259.

Baude A., Bleasdale C., Dalezios Y., Somogyi P. and Klausberger T. (2007). Immunoreactivity for the GABAA receptor alpha1 subunit, somatostatin and Connexin36 distinguishes axoaxonic, basket, and bistratified interneurons of the rat hippocampus. Cereb. Cortex 17, 2094-2107.

Belluardo N., Mudò G., Trovato-Salinaro A., Le Gurun S., Charollais A., Serre-Beinier V., Amato G., Haefliger J.A., Meda P. and Condorelli D.F. (2000). Expression of connexin36 in the adult and developing rat brain. Brain Res. 865, 121-138.

Bennett M.V. and Zukin R.S. (2004). Electrical coupling and neuronal synchronization in the mammalian brain. Neuron 41, 495-511.

Brusco J., Merlo S., Ikeda É.T., Petralia R.S., Kachar B., Rasia-Filho A.A. and Moreira J.E. (2014). Inhibitory and multisynaptic spines, and hemispherical synaptic specialization in the posterodorsal medial amygdala of male and female rats. J. Comp. Neurol. 522, 2075-2088.

Bukalo O., Campanac E., Hoffman D.A. and Fields R.D. (2013). Synaptic plasticity by antidromic firing during hippocampal network oscillations. Proc. Natl. Acad. Sci. USA 110, 5175-5180.

Bupesh M., Legaz I., Abellán A. and Medina L. (2011). Multiple telencephalic and extratelencephalic embryonic domains contribute neurons to the medial extended amygdala. J. Comp. Neurol. 519, 1505-1525.

Chever O., Pannasch U., Ezan P. and Rouach N. (2014). Astroglial connexin 43 sustains glutamatergic synaptic efficacy. Phil. Trans. Royal Soc. B: Biol. Sci. 369, 20130596.

Choi G.B., Dong H-W., Murphy A.J., Valenzuela D.M., Yancopoulos G.D., Swanson L.W. and Anderson D.J. (2005). Lhx6 delineates a pathway mediating innate reproductive behaviors from the amygdala to the hypothalamus. Neuron 46, 647-660

Connors B.W. and Long M.A. (2004). Electrical synapses in the mammalian brain. Annu. Rev. Neurosci. 27, 393-418.

Coolen L.M., Peters H.J.P.W. and Veening J.G. (1997). Distribution of Fos immunoreactivity following mating versus anogenital investigation in the male rat brain. Neuroscience 77, 1151-1161.

de Olmos J.S., Beltramino C.A. and Alheid G. (2004). Amygdala and extended amygdala of the rat: A cytoarchitectonical, fibroarchitectonical, and chemoarchitectonical survey. In: The rat nervous system. Paxinos G. (ed). Elsevier Academic Press. London. pp 509-603.

De Vries G.J. and Simerly R.B. (2002). Anatomy, development, and function of sexually dimorphic neural circuits in the mammalian brain. In: Hormones, brain and behavior. Pfaff D.W., Arnold A.P., Etgen A.M., Fahrbach S.E. and Rubin R.T. (eds). Academic Press. San Diego. pp 137-191.

Gréco B., Blasberg M.E., Kosinski E.C. and Blaustein J.D. (2003). Response of ERα-IR and ERβ-IR cells in the forebrain of female rats to mating stimuli. Horm. Behav. 43, 444-453.

Griemsmann S., Höft S.P., Bedner P., Zhang J., von Staden E., Beinhauer A., Degen J., Dublin P., Cope D.W., Richter N., Crunelli V., Jabs R., Willecke K., Theis M., Seifert G., Kettenmann H. and Steinhäuser C. (2015). Characterization of panglial gap junction networks in the thalamus, neocortex, and hippocampus reveals a unique population of glial cells. Cereb. Cortex 25, 3420-3433.

Horiguchi K., Kouki T., Fujiwara K., Kikuchi M. and Yashiro T. (2011). The extracelular matrix component laminin promotes gap junction formation in the rat anterior pituitary gland. J. Endocrinol. 208, 225-232.

Hull E.M. and Rodríguez-Manzo G. (2017). Male sexual behavior. In: Hormones, brain, and behavior. Pfaff D.W. and Joëls M. (eds). Academic Press/Elsevier. Oxford. pp. 1-57.

Kotini M., Barriga E.H., Leslie J., Gentzel M., Rauschenberger V., Schambony A. and Mayor R. (2018). Gap junction protein Connexin-43 is a direct transcriptional regulator of N-cadherin *in vivo*. Nature

Commun. 9, 3846.

Kovacs G.G., Yousef A., Kaindl S., Lee V.M. and Trojanowski J.Q. (2018). Connexin-43 and aquaporin-4 are markers of ageing-related tau astrogliopathy (ARTAG)-related astroglial response. Neuropathol Appl Neurobiol. 44, 491-505.

Langer J., Stephan J., Theis M. and Rose C.R. (2012) Gap junctions mediate intercelular spread of sodium between hippocampal astrocytes in situ. Glia 60, 239-252.

Meredith M. and Westberry J.M. (2004). Distinctive responses in the medial amygdala to same-species and different-species pheromones. J. Neurosci. 24, 5719-5725.

Micevych P.E., Matt D.W. and Go V.L.W. (1988). Concentrations of cholecystokinin, substance P, and bombesin in discrete regions of male and female rat brain: sex differences and estrogen effects. Exp. Neurol. 100, 416-425.

Nagy J.I. and Rash J.E. (2017). Cx36, Cx43 and Cx45 in mouse and rat cerebellar cortex: species-specific expression, compensation in Cx36 null mice and co-localization in neurons vs. glia. Eur. J. Neurosci. 46, 1790-1804.

Nagy J.I., Pereda A.E. and Rash J.E. (2018). Electrical synapses in mammalian CNS: Past eras, present focus and future directions. Biochim. Biophys. Acta Biomembr. 1860, 102-123.

Newman S.W. (1999). The medial extended amygdala in male reproductive behavior. A node in the mammalian social behavior network. Ann. NY Acad. Sci. 877, 242-257.

Olucha-Bordonau F.E., Fortes-Marco L., Otero-García M., Lanuza E. and Martínez-García F. (2015). Amygdala: Structure and function. In: The rat nervous system. Paxinos G. (ed). Academic Press. San Diego. pp 441-490.

Pannasch U., Derangeon M., Chever O. and Rouach N. (2012). Astroglial gap junctions shape neuronal network activity. Comm. Integr. Biol. 5, 248-254.

Pannese E. (2015). Neurocytology. Springer International. Basel.

Paxinos G. and Watson C. (2008). The rat brain in stereotaxic coordinates. Academic Press. San Diego.

Pereda A.E. (2016). The variable strength of electrical synapses. Neuron 90, 912-914.

Pereda A.E., Curti S., Hoge G., Cachope R., Flores C.E. and Rash J.E. (2013). Gap junction-mediated electrical transmission: regulatory mechanisms and plasticity. Biochim. Biophys. Acta 1828, 134-146.

Pereno G.L., Balaszczuk V. and Beltramino C.A. (2011). Detection of conspecific pheromones elicits fos expression in GABA and calcium-binding cells of the rat vomeronasal system-medial extended amygdala. J. Physiol. Biochem. 67, 71-85.

Pernelle G., Nicola W. and Clopath C. (2018). Gap junction plasticity as a mechanism to regulate network-wide oscillations. PLoS Comput. Biol. 14, 1006025.

Peters A., Palay S.L. and Webster H. (1991). The fine structure of the nervous system. Oxford University Press. New York.

Petrovich G.D., Canteras N.S. and Swanson L.W. (2001). Combinatorial amygdalar inputs to hippocampal domains and hypothalamic behavior systems. Brain Res. Rev. 38, 247-289.

Petrulis A. (2013). Chemosignals and hormones in the neural control of mammalian sexual behavior. Front. Neuroendocrinol. 34, 255-267.

Pfaus J.G. and Heeb M.M. (1997). Implications of immediate-early gene induction in the brain following sexual stimulation of female and male rodents. Brain Res. Bull. 44, 397-407.

Pogoda K., Kameritsch P., Retamal M.A. and Vega J.L. (2016). Regulation of gap junction channels and hemichannels by phosphorylation and redox changes: a revision. BMC Cell. Biol. 24, 138-150.

Posłuszny A. (2014). The contribution of electrical synapses to field potential oscillations in the hippocampal formation. Front. Neural. Circuits 8, 32.

Quagliotto E., Casali K.R., Dal Lago P. and Rasia-Filho A.A. (2015). Neuropeptides in the posterodorsal medial amygdala modulate central cardiovascular reflex responses in awake male rats. Braz. J. Med. Biol. Res. 48, 128-139.

Rackauskas M., Kreuzberg M.M., Pranevicius M., Willecke K., Verselis V.K. and Bukauskas F.F. (2007). Gating properties of heterotypic gap junction channels formed of connexins 40, 43, and 45. Biophys. J. 92, 1952-1965.

Rash J.E., Pereda A., Kamasawa N., Furman C.S., Yasumura T., Davidson K.G., Dudek F.E., Olson C., Li X. and Nagy J.I. (2004). High-resolution proteomic mapping in the vertebrate central nervous system: close proximity of connexin35 to NMDA glutamate receptor clusters and co-localization of connexin36 with immunoreactivity for zonula occludens protein-1 (ZO-1). J. Neurocytol. 33, 131-151.

Rash J.E., Davidson K.G., Kamasawa N., Yasumura T., Kamasawa M., Zhang C., Michaels R., Restrepo D., Ottersen O.P., Olson C.O. and Nagy J. (2005). Ultrastructural localization of connexins (Cx36, Cx43, Cx45), glutamate receptors and aquaporin-4 in rodent olfactory mucosa, olfactory nerve and olfactory bulb. J. Neurocytol. 34, 307-341.

Rasia-Filho A.A., Dalpian F., Menezes I.C., Brusco J., Moreira J.E. and Cohen R.S. (2012a). Dendritic spines of the medial amygdala: plasticity, density, shape, and subcellular modulation by sex steroids. Histol. Histopathol. 27, 985-1011.

Rasia-Filho A.A., Haas D., de Oliveira A.P., de Castilhos J., Frey R., Stein D., Lazzari V.M., Back F., Pires G.N., Pavesi E., Winkelmann-Duarte E.C. and Giovenardi M. (2012b). Morphological and functional features of the sex steroid-responsive posterodorsal medial amygdala of adult rats. Mini Rev. Med. Chem. 12, 1090-1106.

Rela L. and Szczupak L. (2004). Gap junctions: their importance for the dynamics of neural circuits. Mol. Neurobiol. 30, 341-357.

Saper C.B. (2005). Editorial: An open letter to our readers on the use of antibodies. J. Comp. Neurol. 493, 477-478.

Sätzler K., Söhl L.F., Bollmann J.H., Borst J.G., Frotscher M., Sakmann B. and Lübk J.H. (2002). Three-dimensional reconstruction of a calyx of Held and its postsynaptic principal neuron in the medial nucleus of the trapezoid body. J. Neurosci. 22, 10567-10579.

Schoenfeld T.J., Kloth A.D., Hsueh B., Runkle M.B., Kane G.A., Wang S.S. and Gould E. (2014). Gap junctions in the ventral hippocampal-medial prefrontal pathway are involved in anxiety regulation. J. Neurosci. 34, 15679-15688.

Simerly R.B. (2004). Anatomical substrates of hypothalamic integration. In: The rat nervous system. Paxinos G. (ed). Academic Press. San Diego. pp 335-368.

Stehberg J., Moraga-Amaro R., Salazar C., Becerra A., Echeverría C., Orellana J.A., Bultynck G., Ponsaerts R., Leybaert L., Simon F., Sáez J.C. and Retamal M.A. (2012). Release of gliotransmitters through astroglial connexin 43 hemichannels is necessary for fear memory consolidation in the basolateral amygdala. FASEB J. 26, 3649-3657.

Tao-Cheng J-H., Gallant P.E., Brightman M.W., Dosemeci A. and Reese T.S. (2007). Structural changes at synapses after delayed perfusion fixation in different regions of the mouse brain, J. Comp.

Neurol. 501, 731-740.

Theis M. and Giaume C. (2012). Connexin-based intercelular communication and astrocyte heterogeneity. Brain Res. 1487, 88-98.

Tong X., Lopez W., Ramachandran J., Ayad W.A., Liu Y., Lopez-Rodriguez A., Harris A.L. and Contreras J.E. (2015). Glutathione release through connexin hemichannels: Implications for chemical modification of pores permeable to large molecules. J. Gen. Physiol. 146, 245-254.

Wang Y. and Belousov A.B. (2011). Deletion of neuronal gap junction protein connexin 36 impairs hippocampal LTP. Neurosci. Lett. 502, 30-32.

Wu X.L., Tang Y.C., Lu Q.Y., Xiao X.L., Song T.B. and Tang F.R. (2015). Astrocytic Cx 43 and Cx 40 in the mouse hippocampus during and after pilocarpine-induced status epilepticus. Exp. Brain. Res. 233, 1529-1539.

Zancan M., Dall'Oglio A., Sarzenski T.M., Maher M.I., Garcia-Segura L.M. and Rasia-Filho A.A. (2015) Glial and axonal perikaryal coverage and somatic spines in the posterodorsal medial amygdala of male and cycling female rats. J. Comp. Neurol. 523, 2127-2137.

Zancan M., da Cunha R.S.R., Schroeder F., Xavier L.L. and Rasia-Filho A.A. (2018). Remodeling of the number and structure of dendritic spines in the medial amygdala: From prepubertal sexual dimorphism to puberty and effect of sexual experience in male rats. Eur. J. Neurosci. 48, 1851-1865.

Accepted September 9, 2019